

Power Flow Control of Magnetic Resonance Wireless Charging for Hybrid Energy Storage System of Electric Vehicles Application

Katsuhiro Hata^{1†}, Xiaoliang Huang¹, Yoichi Hori¹

¹Graduate School of Frontier Sciences, The University of Tokyo, Chiba, Japan
(Tel: +81-4-7136-3873; E-mail: hata@hflab.k.u-tokyo.ac.jp)

Abstract: Battery and supercapacitor (SC) hybrid energy storage system (HESS) has been widely known for solving a power density problem of a conventional battery storage system for electric vehicles (EVs). Wireless power transfer (WPT) is a promising solution for the EV charging. In this paper, the frame of wireless charging is given for EV applications and a charging power control method for the HESS to achieve the constant current charging of the main battery is proposed. A small power test equipment is implemented and the effectiveness of the charging power control is verified by the experiment. This result shows the importance of the SC bank for the WPT charging system and the need for optimized power coordination control of the HESS.

Keywords: electric vehicle, hybrid energy storage system, wireless charging, charging power control

1. INTRODUCTION

Energy storage systems (ESSs) have been a major research area in electric, hybrid electric and plug-in hybrid electric vehicles (EVs, HEVs, and PHEVs). A battery and supercapacitor (SC) hybrid energy storage system (HESS) is designed to achieve high power density and high energy density in only one system to satisfy the requirement of an EV power train system.

Considering two energy sources among different types such as fuel cells, batteries, SCs and so on, the aim is to achieve high efficiency, high performance, and easy charging of ESSs for EV applications. By applying the HESS to EVs, the battery life can be extended and acceleration performance can be improved [1, 2]. More importantly, efficiency of energy recovery from regenerative braking can be increased based on the characteristics of the SC charging [3].

Wireless power transfer (WPT) can simplify charging operations of EVs. Inductive power transfer and magnetic resonance coupling have been two mainstream methods for applying WPT to an EV charger. WPT via magnetic resonance coupling can achieve a highly efficient mid-range transmission [4]. This characteristics is suitable for a personal EV in terms of a transmitting distance and a misalignment between a transmitter in the ground and a receiver under the vehicle body. Due to a repetitive charging and a dynamic charging for EVs, WPT can reduce the size of the HESS [5] and extend the driving range of EVs [6].

In this paper, the frame of wireless charging for the HESS is given for EV applications. The principle of the power flow regulation to achieve high energy efficiency and to reduce the size of the HESS is discussed. The charging power control of the WPT charger to achieve the constant current charging of the main battery is proposed. A small power test equipment is implemented and the effectiveness of the charging power control is verified by experiment.

[†] Katsuhiro Hata is the presenter of this paper.

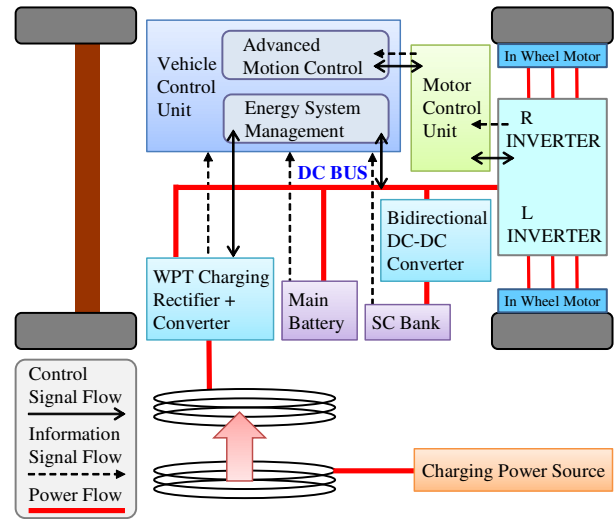


Fig. 1 EV frame powered by HESS with WPT charger.

2. EV STRUCTURE

Fig. 1 shows the EV structure powered by the HESS with the WPT charger. All power devices of the EV are linked by the DC bus and the DC bus voltage is regulated by the main battery. When the power train system requires high power output, the boost converter is commonly connected to the battery. On the other hand, in the small scale EV, the battery can be linked to the DC bus directly. Then, the power flow between the battery, the SC bank, the power train system, and the wireless charging system can be assumed as the current flow of the DC bus. As a result, the current distribution determines the power flow and it is the main control objective for every power converter interface. Therefore, the power flow control can be considered the same as the current control if the DC bus voltage is robust with respect to the output current to the motor traction system and to the charging current from the wireless charging system regarded disturbances.

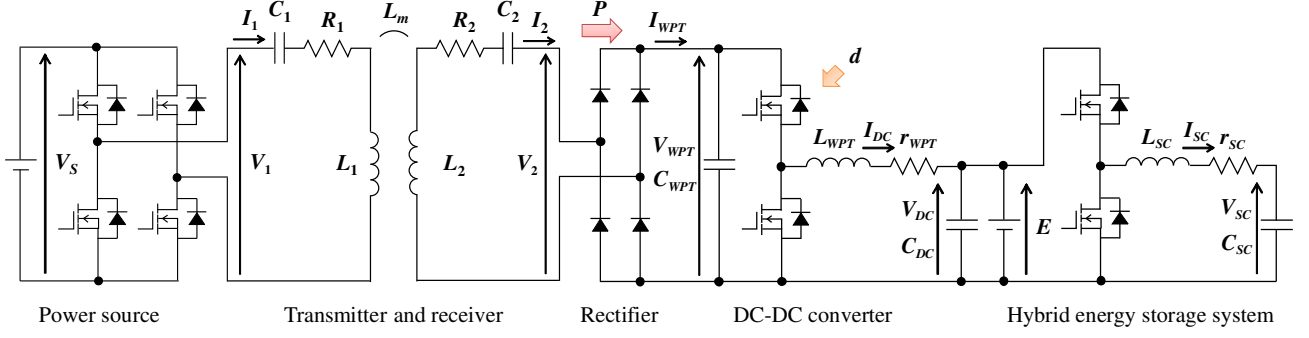


Fig. 2 The whole frame of HESS with WPT charger.

In order to satisfy the power requirements of the EV power train system, frequency decoupling is used as a simple and effective power sharing method [7]. The SC bank provides high frequency output power, while the battery output power becomes smooth. As a result, the maximum output peak power of the ESS can be increased. Additionally, the battery stress can be mitigated and the battery life can be extended naturally.

Setting the SC bank to absorb all regenerative energy can increase the total energy efficiency in comparison with the conventional battery storage system because the SC equivalent series resistance is much lower than the battery one. In addition, the SC bank can be operated as a bidirectional energy interface [3]. Considering the dynamic charging, it can absorb the charging energy from the WPT side and provide the constant power to the power train system at the same time. Therefore, the advantages of the SC are remarkable and will increase the whole system efficiency.

The whole frame of the HESS with the WPT charger is shown in Fig. 2. In this paper, the power train system is neglected as this is a fundamental study. WPT via magnetic resonance coupling uses LC resonance in the transmitter and the receiver. The power source operating frequency is set to the resonance frequency. The transmitting power charges the HESS and its power level is controlled by a DC-DC converter on the WPT side. The charging power can be distributed by a power converter interface for the SC bank. The objective is to achieve the constant current charging of the main battery.

3. WIRELESS CHARGING

3.1. WPT via magnetic resonance coupling

WPT is a promising solution for EV charging. A series-series (SS) circuit topology of WPT via magnetic resonance coupling is used and its equivalent circuit is shown in Fig. 3 [8]. The transmitter and the receiver are characterized by the inductances L_1, L_2 , the series-resonance capacitances C_1, C_2 , and the internal resistances R_1, R_2 respectively. The equivalent resistance R_L includes the power converter interface for the WPT charger. This study focuses on fundamental waves of the primary voltage V_1 and the secondary voltage V_2 to analyze the transmitting efficiency and the charging power.

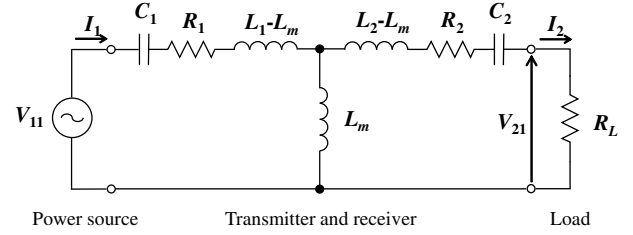


Fig. 3 Equivalent circuit of wireless power transfer.

The primary voltage V_1 and the secondary voltage V_2 can be assumed as rectangular waves and the primary current I_1 and the secondary current I_2 can be approximated as sinusoidal waves in the SS circuit topology of WPT via magnetic resonance coupling [9]. From Fourier series expansion, a fundamental primary voltage V_{11} and a fundamental secondary voltage V_{21} are expressed as follows:

$$V_{11} = \frac{2\sqrt{2}}{\pi} V_S \quad (1)$$

$$V_{21} = \frac{2\sqrt{2}}{\pi} V_{WPT}. \quad (2)$$

If the power source angular frequency ω_0 satisfies eq. (3), a voltage ratio A_V and a current ratio A_I between the transmitter and the receiver are given as eq. (4) and (5).

$$\omega_0 = \frac{1}{\sqrt{L_1 C_1}} = \frac{1}{\sqrt{L_2 C_2}} \quad (3)$$

$$A_V = \frac{V_{21}}{V_{11}} = j \frac{\omega_0 L_m R_L}{R_1 R_2 + R_1 R_L + (\omega_0 L_m)^2} \quad (4)$$

$$A_I = \frac{I_2}{I_1} = j \frac{\omega_0 L_m}{R_2 + R_L} \quad (5)$$

From eq. (4) and (5), the transmitting efficiency η is expressed as follows:

$$\eta = \frac{(\omega_0 L_m)^2 R_L}{(R_2 + R_L) \{R_1 R_2 + R_1 R_L + (\omega_0 L_m)^2\}} \quad (6)$$

and the charging power P is described as follows:

$$P = \frac{(\omega_0 L_m)^2 R_L}{\{R_1 R_2 + R_1 R_L + (\omega_0 L_m)^2\}^2} V_{11}^2. \quad (7)$$

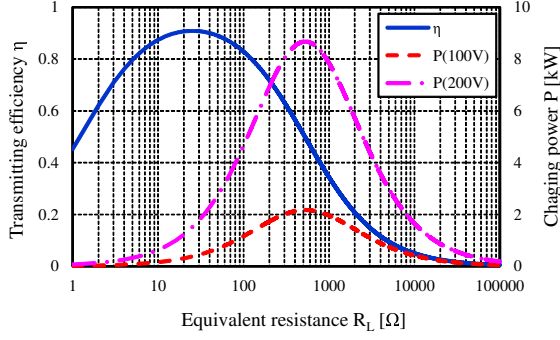


Fig. 4 Equivalent resistance vs. transmitting efficiency and charging power.

Table 1 Parameters of transmitter and receiver.

	Primary coil	Secondary coil
Resistance R_1, R_2	1.15 Ω	1.20 Ω
Inductance L_1, L_2	636 μH	637 μH
Capacitance C_1, C_2	4000 pF	3994 pF
Resonance frequency f_1, f_2	99.8 kHz	99.8 kHz
Mutual inductance L_m		80.8 μH
Coupling coefficient k		0.127
Transmitting gap g		200 mm
Outer diameter		448 mm
Number of turns		56 turns

Fig. 4 shows the equivalent resistance R_L versus the transmitting efficiency η and the charging power P . The parameters of the transmitter and the receiver are listed in Table 1. η is maximized if R_L is given as follows:

$$R_{L\eta\max} = \sqrt{R_2 \left\{ \frac{(\omega_0 L_m)^2}{R_1} + R_2 \right\}}. \quad (8)$$

On the other hand, P is maximized if R_L satisfies the following equation.

$$R_{LP\max} = \frac{(\omega_0 L_m)^2}{R_1} + R_2 \quad (9)$$

Then, the maximum power P_{\max} is given as follows:

$$P_{\max} = \frac{V_{11}^2}{4R_1 \left(1 + \frac{R_1 R_2}{\omega_0 L_m} \right)}. \quad (10)$$

If we can assume $R_1 R_2 \ll \omega_0 L_m$, the maximum power can be approximated as follows:

$$P_{\max} \simeq \frac{V_{11}^2}{4R_1}. \quad (11)$$

Therefore, if the fundamental primary voltage V_{11} is sufficient and the desired power is smaller than P_{\max} , the charging power P can be controlled by the equivalent resistance conversion.

3.2. Charging power control of WPT charger

In order to achieve the constant current charging of the main battery, the charging power should be controlled. However, the current control of the DC–DC converter on the WPT side destabilizes V_{WPT} in Fig. 2. This is because the WPT charger is connected to the constant

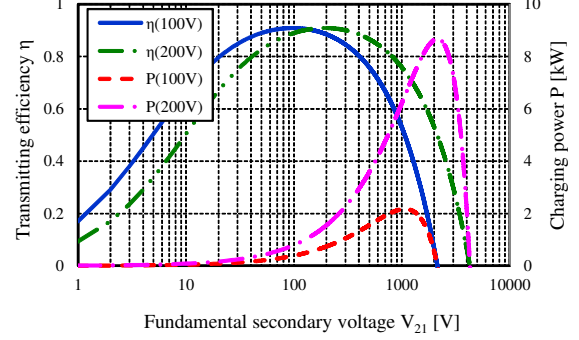


Fig. 5 Fundamental secondary voltage vs. transmitting efficiency and charging power.

power load and the dynamics of V_{WPT} has a unstable pole [10]. Therefore, this paper uses the voltage control of the DC–DC converter on the WPT side for the charging power control [9, 11].

From circuit equations in Fig. 3, the secondary current I_2 can be calculated. Then, the charging power P can be given as follows:

$$P = \frac{\omega_0 L_m V_{11} V_{21} - R_1 V_{21}^2}{R_1 R_2 + (\omega_0 L_m)^2}. \quad (12)$$

Fig. 5 shows the fundamental secondary voltage V_{21} versus the transmitting efficiency η and the charging power P . The parameters of the transmitter and the receiver are described in Table 1. If V_{21} can be controlled, the charging power P can also be controlled. Then, in terms of the transmitting efficiency, V_{21} should be limited below $V_{21P\max}$, which maximize the charging power P and is expressed as follows:

$$V_{21P\max} = \frac{\omega_0 L_m}{2R_1} V_{11}. \quad (13)$$

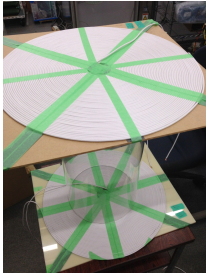
From eq. (12), the reference voltage V_{21}^* , which obtains the desired power P^* , is given as follows:

$$V_{21}^* = \left(\frac{\omega_0 L_m V_{11}}{2R_1} \right) - \sqrt{\left(\frac{\omega_0 L_m V_{11}}{2R_1} \right)^2 - \frac{\{R_1 R_2 + (\omega_0 L_m)^2\} P^*}{R_1}}. \quad (14)$$

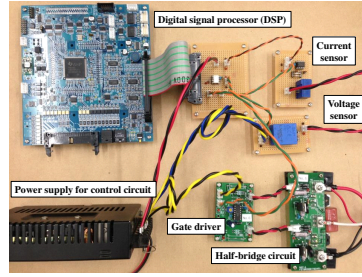
From eq. (2), this is replaced with the DC reference voltage V_{WPT}^* , which is expressed as follows:

$$V_{WPT}^* = \frac{\pi}{2\sqrt{2}} V_{21}^*. \quad (15)$$

As for the voltage control, the DC–DC converter model is analyzed and the control system is designed by the pole placement method [11]. Then, the equilibrium point of the DC–DC converter is defined according to the desired power P^* and the current I_{WPT} . As a result, the duty cycle d of the DC–DC converter can be obtained and the charging power control can be achieved.



(a) Transmitter and receiver.



(b) DC-DC converter.

Fig. 6 Experimental equipment.

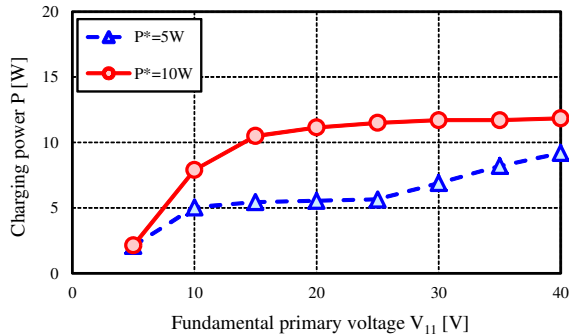


Fig. 7 Experimental result of charging power control.

4. EXPERIMENT

The experimental equipment is shown in Fig. 6. The parameters of the transmitter and the receiver are listed in Table 1. The DC-DC converter was controlled by a digital signal processor. The battery voltage was 12 V and V_{WPT} was controlled by the DC-DC converter.

The experimental result is shown in Fig. 7. When the fundamental primary voltage V_{11} is insufficient, the charging power P is limited by eq. (10). This problem can be avoided by designing the minimum value of V_{11} . On the other hand, when the V_{11} is enough large but the desired power P^* is lower, P^* cannot be achieved because the minimum value of V_{WPT} and P was determined by the battery voltage. If the surplus power can be absorbed into the SC bank, the constant current charging of the main battery can be achieved.

5. CONCLUSION

This paper proposed the charging power control method for the HESS to achieve the constant current charging of the main battery. Experimental result showed the importance of the SC bank for WPT charging and the need for the optimized power coordination control of the HESS with the WPT charger.

In future works, the WPT charging of the HESS using the power coordination control will be experimented and the optimization of the charging power based on information of the HESS will be discussed.

REFERENCES

- [1] J. Cao and A. Emadi, "A new battery/ultracapacitor hybrid energy storage system for electric, hybrid, and plug-in hybrid electric vehicles," *IEEE Transactions on Power Electronics*, vol. 27, no. 1, pp. 122–132, Jan, 2012.
- [2] R. Carter, A. Cruden, and P. J. Hall, "Optimizing for efficiency or battery life in a battery/supercapacitor electric vehicle," *IEEE Transactions on Vehicular Technology*, vol. 61 no. 4, pp.1526–1533, May 2012.
- [3] P. J. Grbovic, P. Delarue, P. L. Moigne, and P. Bartholomeus, "A bidirectional three-level DC-DC converter for the ultracapacitor applications," *IEEE Transactions on Industrial Electronics*, vol. 57, no. 10, pp. 3415–3430, Oct, 2012.
- [4] A. Kurs, A. Karalis, R. Moffatt, J. D. Joannopoulos, P. Fisher, and M. Soljacic, "Wireless power transfer via strongly coupled magnetic resonance," *Science Express on 7 June 2007*, vol. 317, no. 5834, pp. 83–86, Jun. 2007.
- [5] T. Hiramatsu, X. Huang, and Y. Hori, "Capacity design of supercapacitor battery hybrid energy storage system with repetitive charging via wireless power transfer," in *Proc. IEEE 16th International Power Electronics and Motion Control Conference*, 2014, pp. 578–583.
- [6] S. Chopra and P. Bauer, "Driving range extension of EV with on-road contactless power transfer—a case study," *IEEE Transactions on Industrial Electronics*, vol. 60, no. 1, pp. 329–338, Jan, 2013.
- [7] X. Huang, J. M. Curti, and Y. Hori, "Energy management strategy with optimized power interface for the battery supercapacitor hybrid system of electric vehicles," in *Proc. 39th Annual Conference of the IEEE Industrial Electronics Society*, 2013, pp. 4635–4640.
- [8] T. Imura and Y. Hori, "Maximizing air gap and efficiency of magnetic resonant coupling for wireless power transfer using equivalent circuit and Neumann formula," *IEEE Transactions on Industrial Electronics*, vol. 58, no. 10, pp. 4746–4752, Oct. 2011.
- [9] T. Hiramatsu, X. Huang, M. Kato, T. Imura, and Y. Hori, "Wireless charging power control for HESS through receiver side voltage control," in *Proc. 30th annual IEEE Applied Power Electronics Conference and Exposition*, 2015, pp. 1614–1619.
- [10] D. Gunji, T. Imura, and H. Fujimoto, "Stability analysis of secondary load voltage on wireless power transfer using magnetic resonance coupling for constant power load," in *Proc. 2014 IEE of Japan Industry Applications Society Conference*, 2014, pp. 139–142. (in Japanese)
- [11] K. Hata, T. Imura, and Y. Hori, "Dynamic wireless power transfer system for electric vehicle to simplify ground facilities – power control based on vehicle-side information –," in *Proc. 28th International Electric Vehicle Symposium and Exhibition*, 2015, pp. 1–12.